Journal of Quantitative Spectroscopy & Radiative Transfer 164 (2015) 221–230

Contents lists available at ScienceDirect

Journal of Quantitative Spectroscopy & Radiative Transfer

journal homepage: www.elsevier.com/locate/jqsrt

Application of the Hartmann–Tran profile to analysis of H_2O spectra

D. Lisak [a,*], A. Cygan [a], D. Bermejo [b], J.L. Domenech [b], J.T. Hodges [c], H. Tran [d]

[a] Institute of Physics, Faculty of Physics, Astronomy and Informatics, Nicolaus Copernicus University in Torun, Grudziadzka 5, 87-100 Torun, Poland
[b] Instituto de Estructura de la Materia, IEM-CSIC, Serrano 123, 28006 Madrid, Spain
[c] National Institute of Standards and Technology, 100 Bureau Drive, Gaithersburg, MD 20899, USA
[d] Laboratoire Interuniversitaire des Systèmes Atmosphériques, UMR CNRS 7583, Université Paris Est Créteil (UPEC), Université Paris Diderot (UPD), Institut Pierre-Simon Laplace, 94010 Créteil Cedex, France

ARTICLE INFO

Article history:
Received 18 May 2015
Received in revised form
6 June 2015
Accepted 9 June 2015
Available online 20 June 2015

Keywords:
Isolated line shape
Hard collision
Quadratic speed dependence
internal-state changes correlation
PCqSDHC profile
Hartmann–Tran profile

ABSTRACT

The Hartmann–Tran profile (HTP), which has been recently recommended as a new standard in spectroscopic databases, is used to analyze spectra of several lines of H_2O diluted in N_2, SF_6, and in pure H_2O. This profile accounts for various mechanisms affecting the line-shape and can be easily computed in terms of combinations of the complex Voigt profile. A multi-spectrum fitting procedure is implemented to simultaneously analyze spectra of H_2O transitions acquired at different pressures. Multi-spectrum fitting of the HTP to a theoretical model confirms that this profile provides an accurate description of H_2O line-shapes in terms of residuals and accuracy of fitted parameters. This profile and its limiting cases are also fit to measured spectra for three H_2O lines in different vibrational bands. The results show that it is possible to obtain accurate HTP line-shape parameters when measured spectra have a sufficiently high signal-to-noise ratio and span a broad range of collisional-to-Doppler line widths. Systematic errors in the line area and differences in retrieved line-shape parameters caused by the overly simplistic line-shape models are quantified. Also limitations of the quadratic speed-dependence model used in the HTP are demonstrated in the case of an SF_6 broadened H_2O line, which leads to a strongly asymmetric line-shape.

1. Introduction

In recent papers [1–4] the partially Correlated quadratic-Speed-Dependent Hard-Collision profile (pCqSDHCP) was proposed as a standard model for isolated line-shapes to go beyond the widely used Voigt profile in spectroscopic databases and radiative transfer calculations. This profile is a version of the correlated speed-dependent Rautian profile of Pine [5] with the speed-dependence of collisional width and shift given in the quadratic form proposed by Rohart et al. [6,7]. The pCqSDHCP, which is also widely known as the partially Correlated quadratic-Speed-Dependent Nelkin–Ghatak profile (pCqSDNGP), was recently recommended in Ref. [8] as a standard profile, where it was proposed to be called the Hartmann–Tran profile (HTP). Indeed, the Voigt profile does not allow us to fully exploit tremendous advances in spectroscopic instrumentation [9–11] and it cannot fulfill the increasingly demanding precision requirements in Earth observation missions (e.g. [12–15]). Several non-Voigt effects on the line-shape must be taken into account in order to accurately describe the measured spectra. In [1], we have shown that the HTP can reproduce the

* Corresponding author. Tel.: +48 566113282.
E-mail address: dlisak@fizyka.umk.pl (D. Lisak).

http://dx.doi.org/10.1016/j.jqsrt.2015.06.012
0022-4073/

spectral line shapes of different molecular systems within a few parts-per-thousand at atmospheric pressure conditions (from low pressure up to 1 atm). This profile accounts for various non-Voigt effects on the spectral shape through well-identified line-by-line parameters: velocity changes due to collisions (i.e. the Dicke narrowing effect), speed dependencies of the broadening and shifting parameters and correlation between velocity and internal-state changes. Recently the HTP was fit to high signal-to-noise ratio spectra of CO_2 [16] and H_2O [17], which illustrated the utility of the HTP and showed the importance of non-Voigt mechanisms on line-shape. Importantly, we have shown that this profile can be written as combinations of the complex Voigt function and hence can be quickly and easily computed. Its use is thus compatible with the analysis of laboratory measurements and atmospheric spectra.

In the remainder of this paper, we quantify the extent to which the HTP can model self- and foreign-broadened water vapor line shapes for various ranges of pressure and spectrum signal-to-noise ratios. To this end, we fit the HTP and other parameterized line-shape models to theoretically calculated (see [1]) and measured water vapor spectra using a multi-spectrum fitting technique, and we quantify fit residuals and systematic differences in retrieved line parameters. Measurements are based on two sets of cavity ring-down spectroscopy (CRDS) spectra for transitions in the $2\nu_1+\nu_3$ and $4\nu_2$ bands near $10,687\ \mathrm{cm}^{-1}$ and $6245\ \mathrm{cm}^{-1}$, respectively, and on difference frequency generation (DFG) absorption spectra for a transition in the ν_3 band near $3838\ \mathrm{cm}^{-1}$. Perturbers considered include N_2, SF_6 and H_2O. These results allow us to evaluate the systematic errors resulting from the use of simplified line-shape models. A similar study of O_2 was also recently done by comparing *ab initio* line shape calculations with a variety of semiclassical models [18].

2. Data used and analysis procedure

In order to quantify how the quality-of-fit (QF) [9,16] and biases in fitted line-shape parameters depend on the choice of line profile, spectra need to span a wide range of pressures and have a sufficiently high signal-to-noise ratio (SNR). This is because at a given pressure, there can be numerical correlations between parameters that result in similar changes to the line-shape. For example, the effects of velocity-changing collisions and speed-dependence of the collisional width both lead to reduction in line width. However these two line-narrowing mechanisms affect the Doppler and collisional components of the line shape, respectively, and therefore they can be distinguished by simultaneously fitting a properly constrained line profile to spectra acquired over pressures covering both the Doppler- and collisional-dominated domains.

First, the analysis of simulated spectra of the $4_{04}-3_{03}$ line from the ν_3 band of H_2O perturbed by N_2 (see Ref. [1]) was extended to several commonly used semiclassical line shapes. These simulated spectra were analyzed by multi-spectrum fits for a wide range of the Lorentz-to-Doppler width ratio (Γ/Γ_D) and resulted in conclusions which were verified by subsequent analysis of the measured spectra. In this case, the simulated spectra have Γ/Γ_D between 0.17 and 19.7, which corresponds to pressures from 9 hPa to 1040 hPa. Recall that these theoretical line-shape simulations were done with the Keilson–Storer model of velocity changes and semi-classical calculations of the speed-dependent line widths and shifts. Details can be found in Ref. [19], where a high level of agreement between these simulated and measured spectra was found.

The results and conclusions obtained from simulated spectra were then verified by fitting line profiles to measured spectra. Specifically, spectra of the $\nu_3 4_{04}-3_{03}$ line ($\nu_0 = 3837.869\ \mathrm{cm}^{-1}$) of H_2O perturbed by N_2 were measured using DFG laser absorption spectroscopy. These data were acquired at 298 K and at 9 pressures between 100 hPa and 1200 hPa [20] leading to collisional-to-Doppler width ratios Γ/Γ_D of 1.8–23. The SNR of these experimental spectra is between 600 and 1400.

The second set of measured spectra is of the $4_{04}-3_{03}$ line in the $2\nu_1+\nu_3$ band ($\nu_0 = 10,687.326\ \mathrm{cm}^{-1}$) of H_2O perturbed by N_2. These spectra were measured with the frequency-stabilized cavity ring-down spectroscopy (FS-CRDS) technique at 295.8 K and for 4 pressures between 67 hPa and 533 hPa [21], which leads to Γ/Γ_D of 0.45–3.6. For each pressure, two spectra were measured with SNRs between 400 and 720. The third set of spectra considered here were for the same water transition diluted in SF_6 [21]. This relatively heavy perturber (8.11 times the mass of H_2O) is particularly interesting because the influence of the speed-dependent effects on observed line shape typically increases with perturber-to-absorber mass ratio [22]. In this case, spectra were measured at 295.1 K, at four pressures between 67 hPa and 533 hPa with SNRs between 320 and 710. The ratio Γ/Γ_D for these data spans from 0.37 to 2.9.

The fourth set of measured spectra is for the self-broadened H_2O $5_{14}-5_{05}$ line in the $4\nu_2$ vibrational band ($\nu_0 = 6244.7193\ \mathrm{cm}^{-1}$). This line was measured using CRDS at 296 K and for 8 pressures between 1 hPa and 18 hPa [23]. These conditions lead to Γ/Γ_D between 0.046 and 0.83. The achieved SNR ranges from 500 near the line peak to over 10,000 in the line wings.

The most commonly used line-shape models: Voigt profile (VP), Galatry profile – GP (also called the soft-collision profile), Nelkin–Ghatak profile – NGP, speed-dependent Voigt profile – qSDVP, speed-dependent Nelkin–Ghatak profile – qSDNGP, and Hartmann–Tran profile – HTP (which is the partially correlated speed-dependent Nelkin–Ghatak profile – pCqSDNGP) were fit to all simulated and measured spectra. In the last three speed-dependent profiles the quadratic model for the speed-dependence of collisional broadening and shifting [6,7] was applied, as indicated by "q" in the profile acronyms. Additionally, for one data set (line $4_{04}-3_{03}$ from the $2\nu_1+\nu_3$ band of H_2O perturbed by SF_6) profiles using the hypergeometric speed-dependence model [22] were used. These profiles have "h" in their acronyms instead of "q"; namely hSDVP, hSDNGP, pChSDNGP. It should be noted here that the Nelkin–Ghatak profile, based on the hard-collision model of the velocity-changing collisions, is also called hard-collision profile (HCP) and analogous alternative acronyms for the other hard-collision profiles are commonly used, e.g. qSDHCP and pCqSDHCP instead of qSDNGP and pCqSDNGP.

The multi-spectrum fitting procedure used here differs slightly from that used in Ref. [1]. Here we treat the integrated line areas as free parameters for each pressure. This is because, contrary to the case of simulated spectra, for most of these measured spectra, the relative uncertainty in the partial pressure of H_2O is significantly greater than the inverse of the SNR. Therefore, constraining line areas to the expected values would lead to systematic distortions of residuals from the fit. The other line-shape parameters are shared for all pressures. The collisional broadening Γ and shifting Δ, and frequency of the velocity-changing collisions (which leads to Dicke-narrowing and which is called the frequency of optical collisions ν_{opt}) depend on the perturber pressure p. This quantity is well-known experimentally and therefore the linear dependencies on pressure of these quantities, Γ/p, Δ/p, ν_{opt}/p, are fitted. The quadratic speed-dependencies of the collisional width Γ and shift Δ are described by the dimensionless and pressure-independent parameters, a_W and a_S, respectively, see e.g. [24]. The relations of these parameters to the speed-dependent collisional width and shift parameters in the notation used in Refs. [1,3,8], Γ_0, Γ_2, Δ_0, Δ_2, are as follows: $\Gamma = \Gamma_0$, $\Delta = \Delta_0$, $a_W = \Gamma_2/\Gamma_0$, and $a_S = \Delta_2/\Delta_0$. In the case of the hypergeometric speed-dependence, the corresponding fitted parameters are $m_w = (q-3)/(q-1)$ and $n_s = -3/(q-1)$ for speed-dependencies of the width and shift, respectively. They may be interpreted in terms of an exponent q in the absorber–perturber interaction energy which is proportional to the inverse power r^{-q} of the intermolecular distance r. Finally, the parameter η describing correlations between velocity- and phase/state changing collisions is pressure independent.

3. Results and discussion

3.1. Simulated H_2O $\nu_3 4_{04} - 3_{03}$ line

In this section we analyze the influence of the spectra SNR on the ability to obtain non-Voigt line-shape parameters from multi-spectrum fits of the HTP. In Fig. 1 simulated profiles of the H_2O $\nu_3 4_{04} - 3_{03}$ line perturbed by N_2 are presented with residuals from multi-spectrum fits for various line-shape models. Although this line was previously analyzed with the VP and HTP in Ref. [1], the present residuals are slightly different because the individual line areas were varied in the fitting procedure, as explained in Section2. The Voigt profile deviates from the simulated one by up to 2% and the HTP only by less than 0.05%. It is also clear that the simulated line shapes can be better reproduced by assigning the non-Voigt effects to speed-dependent effects (qSDVP) rather than collisional narrowing (GP, NGP). Taking both speed dependence and collisional narrowing into account (qSDNGP) does not improve the fit quality compared to the qSDVP, for which residuals are as much as 0.3%. The same set of spectra were then simulated with the addition of Gaussian white noise. The SNR of the simulated spectra was varied from 250 to 8000 by corresponding adjustment of the noise standard deviation. These spectra were fitted with the HTP, as described above for the case without noise. Instead of visually comparing residuals from the fits for each SNR it is convenient to define the quality of fit (QF) parameter [9], which is defined as the ratio of the peak absorption to the standard deviation of the fit residuals. In the case of a perfect fit QF should be equal to the SNR. In the multi-spectrum fit the QF can be calculated for the whole set of pressures [16].

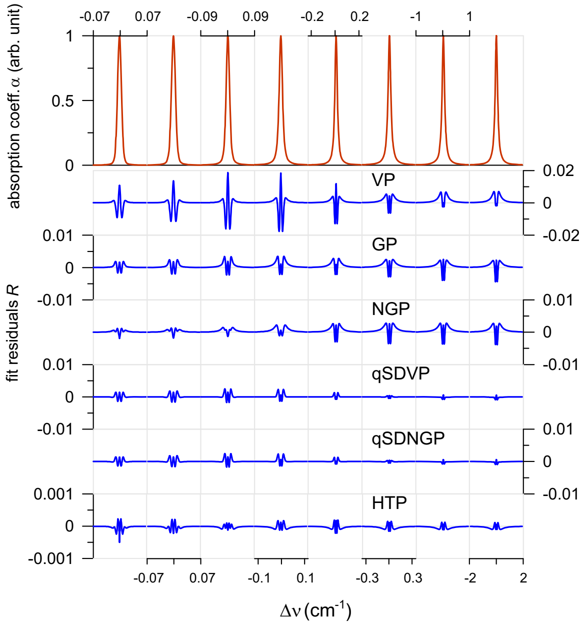

Fig. 1. Simulated profiles of H_2O $\nu_3 4_{04} - 3_{03}$ line perturbed by N_2 and residuals from multi-spectrum fits with various line-shape models. Spectra correspond to gas pressures: 9, 18, 36, 70, 138, 379, 743, and 1040 hPa.

In Fig. 2 the ratios QF/SNR are plotted as a function of SNR for multi-spectrum fits of various profiles. A QF/SNR close to unity corresponds to a nearly perfect fit. The results also depend on the range of the collisional-to-Doppler broadening ratio Γ/Γ_D of the simulated spectra. Fig. 2(a) corresponds to fitting spectra for all pressures (9–1040 hPa), with Γ/Γ_D varying from 0.17 to 19.7. Fig. 2(b) and (c) corresponds to the collisional regime, with $\Gamma/\Gamma_D > 3.7$, and the Doppler regime with $\Gamma/\Gamma_D < 0.35$, respectively. Clearly in the case of a broad range of pressures (Fig. 2(a)) the speed-dependent profiles (qSDVP, qSDNGP) which ignore correlations between velocity- and phase-changing collisions begin to deviate from the reference profile at a SNR greater than 500. Profiles which consider velocity-changing collisions, but not the speed-dependent effects deviate from the reference data even at SNR equal 250. The HTP is able to reproduce the simulated spectra up to a SNR of 4000. These conclusions are in good agrement with comparison of the maximum deviations of the fit residuals of spectra without noise, shown in Fig. 1 for given profiles.

In the case of the collisional regime (Fig. 2(b)) the HTP yields even better fits to the reference spectra. A decrease of the QF/SNR from unity was only 3.1% for a SNR of 8000, compared to 10.6% for a broad range of Γ/Γ_D. Also the two other speed-dependent profiles (qSDVP, qSDNGP) lead to

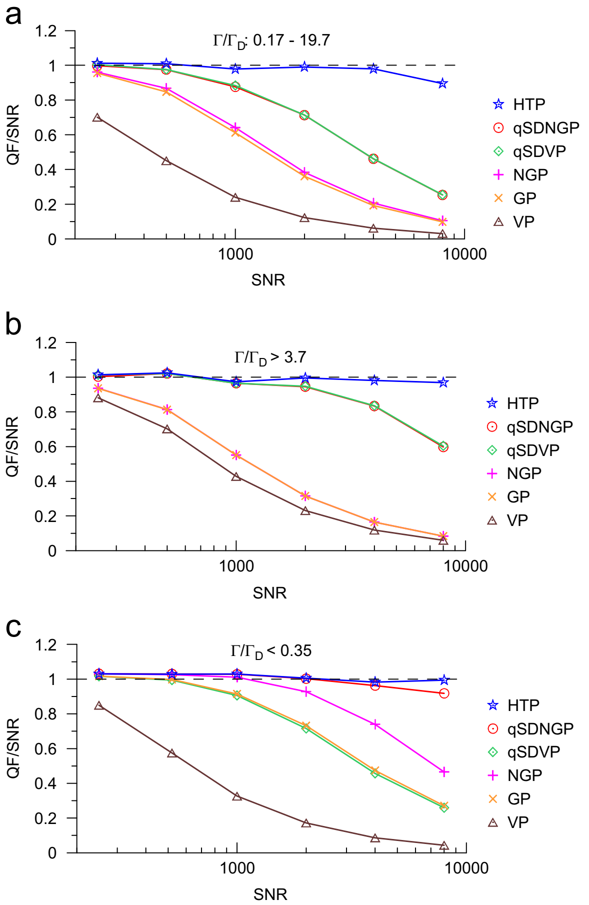

Fig. 2. QF/SNR ratios plotted as a function of SNR for multi-spectrum fits of various profiles to the simulated H_2O $\nu_3 4_{04}-3_{03}$ line perturbed by N_2. Panels (a)–(c) corresponds to various ranges of collisional-to-Doppler width ratios Γ/Γ_D.

near-perfect fits for SNRs up to 1000. This can be explained by the weak influence of velocity-changing collisions when the line-shape is dominated by pressure broadening. A different situation can be observed for the low Γ/Γ_D range, shown in Fig. 2(c). Here, the velocity-changing collisions are more important than the speed-dependent effects for proper description of the line shape. In this case, the NGP can reproduce the simulated spectra with a SNR up to 1000, and the qSDNGP even up to over 2000. The HTP leads to a near-perfect fit for all SNRs considered here. Interestingly the qSDVP fails at a SNR below 500 and this profile leads to the same fit quality as the GP. It was demonstrated earlier [7,25] that at low pressures these two profiles lead to very similar shapes, even if they describe different physical non-Voigt effects.

We used the fits to simulated, noisy spectra to estimate the uncertainties (both precision and systematic effects) in non-Voigt line-shape parameters which would be determined from fits to real spectra. It is expected that these uncertainties will depend on SNR and various ranges of the collisional-to-Doppler width ratio Γ/Γ_D. In Fig. 3 ratios of fitted HTP line-shape parameters for a given SNR to the same parameters obtained from noise-free spectra are

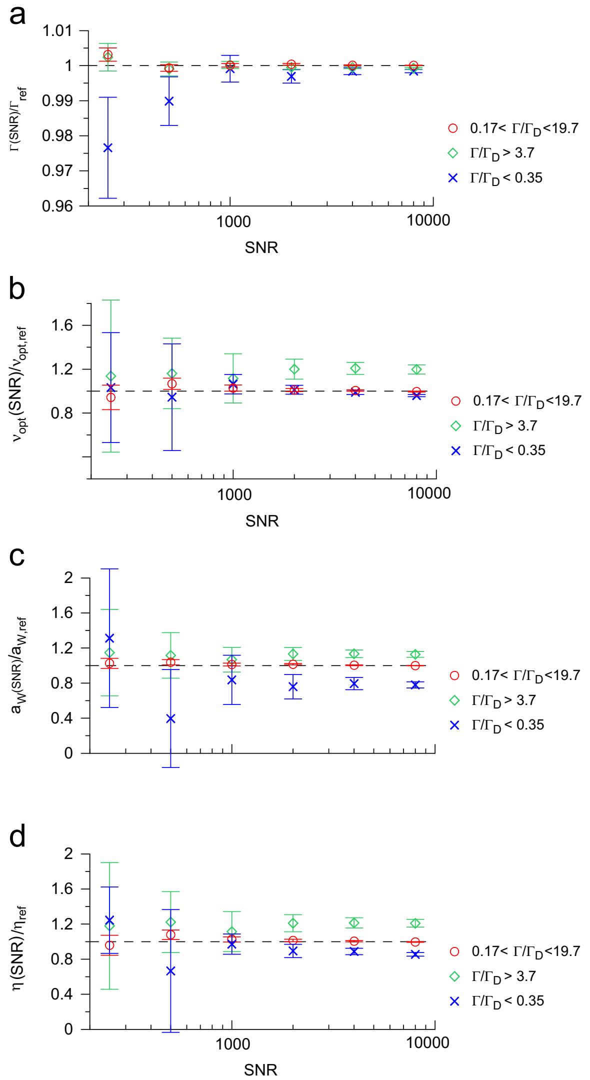

Fig. 3. Ratios of fitted line-shape parameters of HTP for a given SNR to the reference parameters vs. the SNR of the fitted spectra. (a) Collisional broadening Γ, (b) frequency of optical collisions ν_{opt}, (c) quadratic speed-dependence of collisional width a_W, (d) correlations between velocity- and phase/state changing collisions η. Error bars correspond to the standard uncertainty of the fitted parameter ratios. Red circle plots correspond to multi-spectrum fit of all simulated data, with $0.17<\Gamma/\Gamma_D<19.7$; green square plots correspond to the collisional regime ($\Gamma/\Gamma_D>3.7$); blue cross plots correspond to the Doppler regime ($\Gamma/\Gamma_D<0.35$). The reference parameters are obtained from spectra without noise for $0.17<\Gamma/\Gamma_D<19.7$. (For interpretation of the references to color in this figure caption, the reader is referred to the web version of this paper.)

plotted as a function of the SNR of the fitted spectra. Panels (a)–(d) of Fig. 3 present results for the collisional broadening parameter Γ, the frequency of optical collisions ν_{opt}, the quadratic speed-dependence of collisional width a_W, and the parameter describing correlations between velocity- and phase/state changing collisions η.

The advantage of using a multi-spectrum fit that simultaneously covers both the Doppler- and collisional regimes is clearly visible in Fig. 3. The standard uncertainties of all parameters are about an order of magnitude smaller than in the case where the fitted data were limited to low or high Γ/Γ_D ratios. Also it is worth noting that even for the lowest SNR of 250, for which differences between HTP and two other speed-dependent profiles are barely visible in the fit residuals (see Fig. 2(a)), all of the fitted parameters are consistent within their standard uncertainties with results of the fit to the noise-free spectra.

In the case of data sets that are limited to either high or low pressures, the fitted line-shape parameters are systematically different than those retrieved from spectra spanning a broad pressure range. The magnitude of these differences is parameter dependent and is significantly larger than the standard uncertainty of the fitted parameters for the spectra with SNR above 2000. On the other hand for spectra with the lowest SNR (below 500) the uncertainties of the non-Voigt line shape parameters (ν_{opt}, a_W, η) increase to nearly 100% of their values, making their determination impossible.

It should be noted that the present analysis was made for the case where the number of data points in the spectra was significantly larger than the number of fitted parameters. Obviously, the ability to determine the non-Voigt line-shape parameters is also related to the number of data points. In the case of random Gaussian noise, spectra having N-times higher number of uncorrelated data points would be approximately equivalent to increasing the SNR by the factor $\sqrt{N}$.

3.2. Measured H_2O spectra

The results of the simulations described above can be compared with the analysis of measured spectra for the same transition. These measured profiles and fit residuals are presented in Fig. 4. The fit residuals from the VP are up to 1.5%, and their distribution with pressure is slightly different than for the simulated spectra. This is likely because of the different pressure ranges and weighting of the spectra caused by different peak absorptions and spectrum point densities. The limited signal-to-noise ratio of these spectra causes the residuals of the three speed-dependent profiles to look the same. This is consistent with results of the simulation in Fig. 2(b) for line shapes dominated by collisional broadening and a SNR of about 1000. The observations that the VP leads to up to about 2% disagreement and that the qSDVP fits better than GP and NGP are similar to those obtained from the simulated profiles in Fig. 1.

The QF values presented in Fig. 4 confirm that all three speed-dependent profiles can equally well reproduce the experimental data. We note that one should be careful about comparing the QF values for different data sets, because for an imperfect fit QF depends on the length of the measured line wings.

The next set of experimental data, which corresponds to a line with the same rotational quanta but from a different band ($2\nu_1+\nu_3$), is shown in Fig. 5. The ratio of collisional-to-Doppler width is much smaller (0.45–3.6) than in the ν_3 band. The use of the VP leads to about 0.5% of mainly systematic deviations in the fitted spectra,

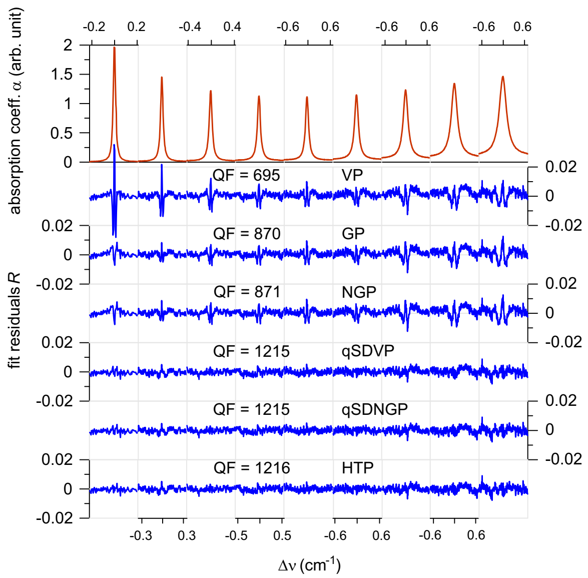

Fig. 4. Measured profiles of the H_2O ν_3 $4_{04}-3_{03}$ line perturbed by N_2 and residuals from multi-spectrum fits with various line-shape models. Spectra correspond to gas pressures: 99, 197, 294, 398, 499, 600, 797, 1000, and 1200 hPa.

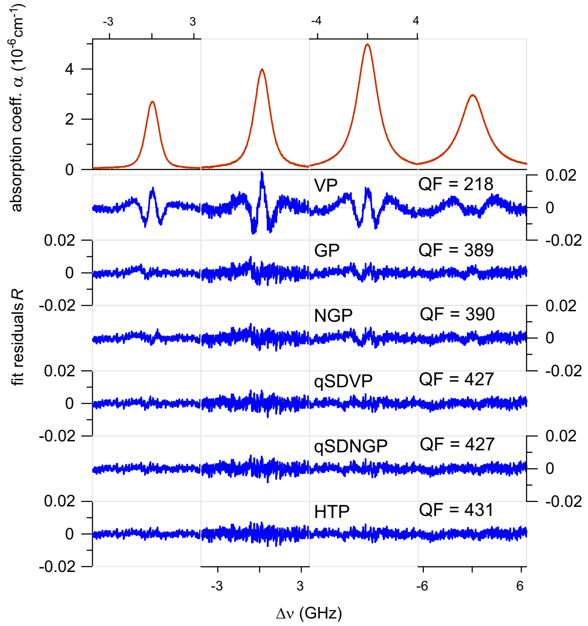

Fig. 5. Measured profiles of H_2O $2\nu_1+\nu_3$ $4_{04}-3_{03}$ line perturbed by N_2 and residuals from multi-spectrum fits with various line-shape models. Spectra correspond to gas pressures: 67, 133, 267, and 533 hPa.

whereas the GP and NGP reduce this deviation to about 0.1%. All three speed-dependent profiles can reproduce the measured spectra to nearly the experimental noise level, but a small improvement of the fit quality at the lowest pressure is visible for the HTP residuals. A more quantitative analysis using the QF factor confirms this conclusion, which is also consistent with results of simulations in Fig. 2. For the range of pressures that covers both $\Gamma<\Gamma_D$ and $\Gamma>\Gamma_D$ the difference between the HTP and the two other speed-dependent profiles is more visible even at lower SNR (about 500) than in the collisionally dominated region of spectra in Fig. 4 at higher SNR (about 1000).

Another set of experimental spectra considered here is the $2\nu_1+\nu_3$ $4_{04}-3_{03}$ line of H_2O perturbed by heavy SF_6 molecules. In this case the relatively large collisional line shifting Δ (6.3 times bigger than for perturbation by N_2) leads to significant line asymmetry caused by the speed-dependence of Δ [21]. Experimental profiles and multi-spectrum fit residuals corresponding to various line-shape models are presented in Fig. 6. Line asymmetry is clearly seen by inspection of the residuals from fits of the symmetric profiles VP, GP, NGP. The maximum residual amplitudes of 2.3% for the GP and NGP are only slightly lower than those of the VP. Unlike the other investigated spectra in the case of perturbation by SF_6 the HTP is not able to reproduce the experimental profiles to within the random noise limit. Therefore, in addition to the three profiles (qSDVP, qSDNGP, HTP) which assume quadratic speed-dependence, spectra were fitted with profiles in which the hypergeometric speed-dependent model was applied (hSDVP, hSDNGP, pChSDNGP). The hypergeometric speed-dependence is more physically justified than quadratic model and was previously reported to give better agreement with measured spectra of H_2O [26]. Also for the case presented in Fig. 6 it is clear that the hypergeometric speed-dependence model can better reproduce the measured spectra than the quadratic model, for which systematic deviations of the residuals are up to about 1%.

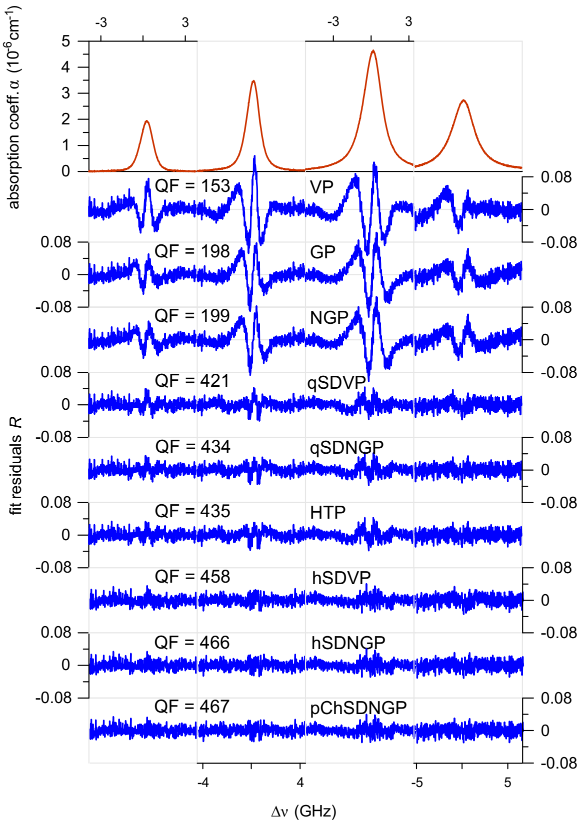

Fig. 6. Measured profiles of H_2O $2\nu_1+\nu_3$ $4_{04}-3_{03}$ line perturbed by SF_6 and residuals from multi-spectrum fits with various line-shape models. Spectra correspond to gas pressures: 67, 133, 267, and 533 hPa.

The last set of spectra shown in Fig. 7 represents a self-broadened H_2O $4\nu_2$ $5_{14}-5_{05}$ line in the case of mostly Doppler-dominated regime ($\Gamma/\Gamma_D<0.83$). For this data it was not possible to fit the HTP, because the fit residuals were too weakly dependent on the correlation parameter η. Therefore our analysis was limited to the uncorrelated model qSDNGP, which is equivalent to the HTP with $\eta=0$. This observation is consistent with results of simulations for the low-pressure case shown in Fig. 2(c) in which the HTP and qSDNGP lead to equal fit qualities up to a SNR of above 2000.

As was demonstrated earlier, see e.g. [16,21,27,28] subpercent deviations of the fit residuals for various model profiles may be associated with significant differences of fitted line parameters and line intensities. In Fig. 8 ratios of the fitted line areas to the reference (the most accurate) areas are shown as a function of perturber pressure. Graphs (a), (b), (c), (d) and (e) of Fig. 8 correspond to the five data sets presented in Figs. 1, 4, 5, 6 and 7, respectively. The reference line areas are based on the exact simulated area (Fig. 8(a)), fitting with the HTP (Fig. 8(b) and (c)), fitting with the pChSDNGP (Fig. 8(d)) and fitting with the qSDNGP (Fig. 8(e)). Systematic errors of the fitted line areas generally increase with perturber pressure. Using the VP always leads to an underestimation of the area and this effect is up to 6% for data considered here. Also the use of GP and NGP causes underestimation of the line areas in most cases, but the effect is smaller than for the VP. Only for asymmetric line $2\nu_1+\nu_3$ $4_{04}-3_{03}$ perturbed by SF_6 (Fig. 8(d)) does the GP give surprisingly good line areas which agree to within 0.25% of the reference values. The speed-dependent profiles with the quadratic model, qSDVP, qSDNGP and HTP, overestimate line areas, which is especially visible in Fig. 8(a) and (d) for which the HTP is not a reference. However, systematic error of line area caused by the use of the HTP is smaller than 0.04% for the N_2-broadened line (Fig. 8(a)) and smaller than 0.5% for the SF_6-broadened line (Fig. 8(d)). For the self-broadened H_2O line at low pressures (Fig. 8(e)) all profiles except for the VP, lead to errors in the line area of less than 0.5%.

We note however that the magnitude of systematic error in the line area depends not only on the simplifications inherent in the line-shape model. This error also depends on the pressure range used in the multi-spectrum fit, the distribution of measured spectra within this pressure range, as well as on the length of the line wings measured for each spectrum. For example, as demonstrated in Ref. [29] in the case of the H_2O $\nu_1+\nu_3$ $3_{22}-2_{21}$ line perturbed by N_2, systematic error associated with the use of the VP varies between 2% and 11% depending on the length of the line wings.

Other line-shape parameters may be much more dependent on the fitted profile than the line area. Ratios of the line-shape coefficients to the corresponding coefficients obtained from the reference model HTP are presented in Fig. 9 for the collisional broadening parameter Γ/p (Fig. 9(a)), the frequency of optical collisions ν_{opt}/p (Fig. 9(b)) and the collisional shifting parameter Δ/p (Fig. 9(c)) for all four data sets considered here. The horizontal axis in Fig. 9 indicates the

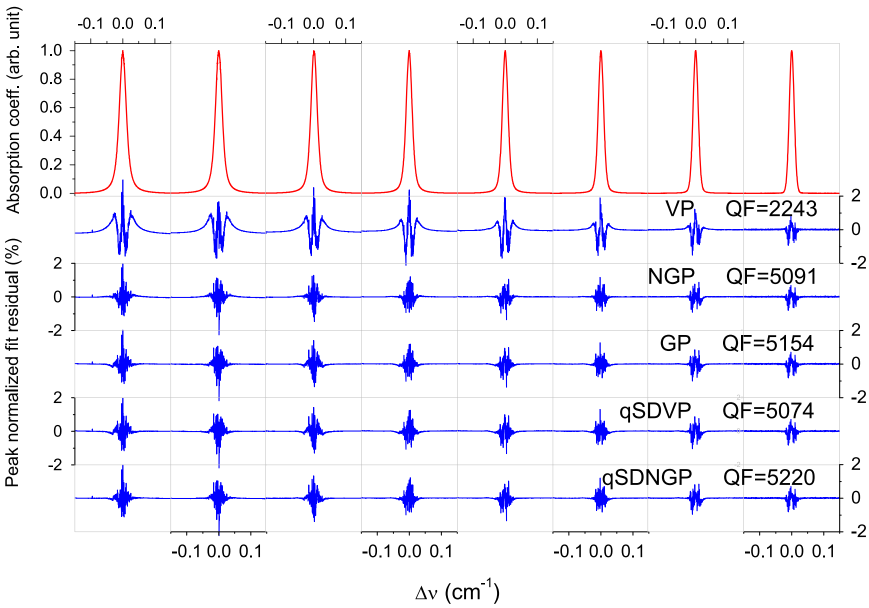

Fig. 7. Experimental profiles of the self-broadened H_2O $4\nu_2$ $5_{14}-5_{05}$ line and residuals from multi-spectrum fits with various line-shape models. Spectra correspond to gas pressures: 18.23, 15.87, 13.3, 10.65, 7.99, 5.33, 2.66, and 0.666 hPa.

fitted line-shape model. These results allow us to quantify the systematic error incurred when line-shape parameters obtained from fits of one profile are used to simulate spectra using a different profile. For example if the collisional width Γ obtained from the VP is used with the HTP, it will cause a 3–9% systematic error in the collisional width. The relative differences between the collisional narrowing parameters ν_{opt} obtained from various profiles (9(b)) are very large and mainly associated with whether or not speed dependent effects are taken into account. In the case of the speed-independent profiles (GP, NGP) the fitted ν_{opt} accounts for both line narrowing mechanisms (the collisional narrowing and speed-dependent effects) and therefore the fitted value is always larger than that obtained from the qSDNGP and hSDNGP. Taking the correlation effect into account (HTP and pChSDNGP) leads to a significant increase in the fitted ν_{opt}, compared to those obtained with the qSDNGP and hSDNGP, for all presented cases.

In the case of collisional shifting Δ the profiles can be divided to two groups: symmetric profiles (VP, GP, NGP) and asymmetric (all speed-dependent profiles). Both groups lead to systematically different Δ values, ranging from 10% to 19%. Even for asymmetric profiles the collisional shift may differ by up to 3% between profiles which use the quadratic and hypergeometric speed dependence model. These systematic errors in the collisional shifting coefficients are crucial to estimating systematic line-shape-induced error in the measurement of unperturbed transition frequency, because this frequency is usually determined from line positions extrapolated to zero pressure.

A complete list of line-shape parameters obtained from the multi-spectrum fits of the HTP to the four data sets studied here is given in Table 1. For the last line $4\nu_2$ $5_{14}-5_{05}$ the parameters of the qSDNGP are reported in Table 1 because it was not possible to fit η from the experimental data. It is worth noting that the fitted collisional narrowing and correlation parameters for the experimental spectra of ν_3 $4_{04}-3_{03}$ line are about half that of the simulated one. This may be associated with the limited signal-to-noise of the measured spectra or the occurrence of asymmetry that cannot be completely described by a quadratic speed dependence of the collisional shift.

4. Conclusions

We have measured non-Voigt line-shape effects in near- and mid-IR H_2O spectra for various physical and experimental conditions, which leads to several general conclusions. The use of the Voigt profile causes several percent deviations in the fit residuals and systematic errors of several percent in the line area. This systematic error typically increases with pressure. Profiles that take into account collision-induced velocity changes effect but not the speed-dependent effects (GP and NGP) usually lead to less than 2% deviations in the fit residuals and line areas. However, for asymmetric lines, like the SF_6 broadened water line presented here where there is a large speed-dependent collisional shift, the magnitude of the fit residuals from the symmetric GP or NGP may be similar to that from VP. The speed-dependent profiles with the quadratic model lead to sub-percent deviations in the fit residuals and fitted line areas.

By incorporating both the speed-dependence and collisional narrowing effects simultaneously in the fitted profile, one can further reduce the fit residuals especially at a low range of collisional-to-Doppler line widths ratios Γ/Γ_D as shown in Fig. 2c. However, a sufficiently high spectrum signal-to-noise ratio (SNR above 1000) is needed to observe improvement of the fit quality for the qSDNGP, compared to the qSDVP. The use of the HTP reduces the fit

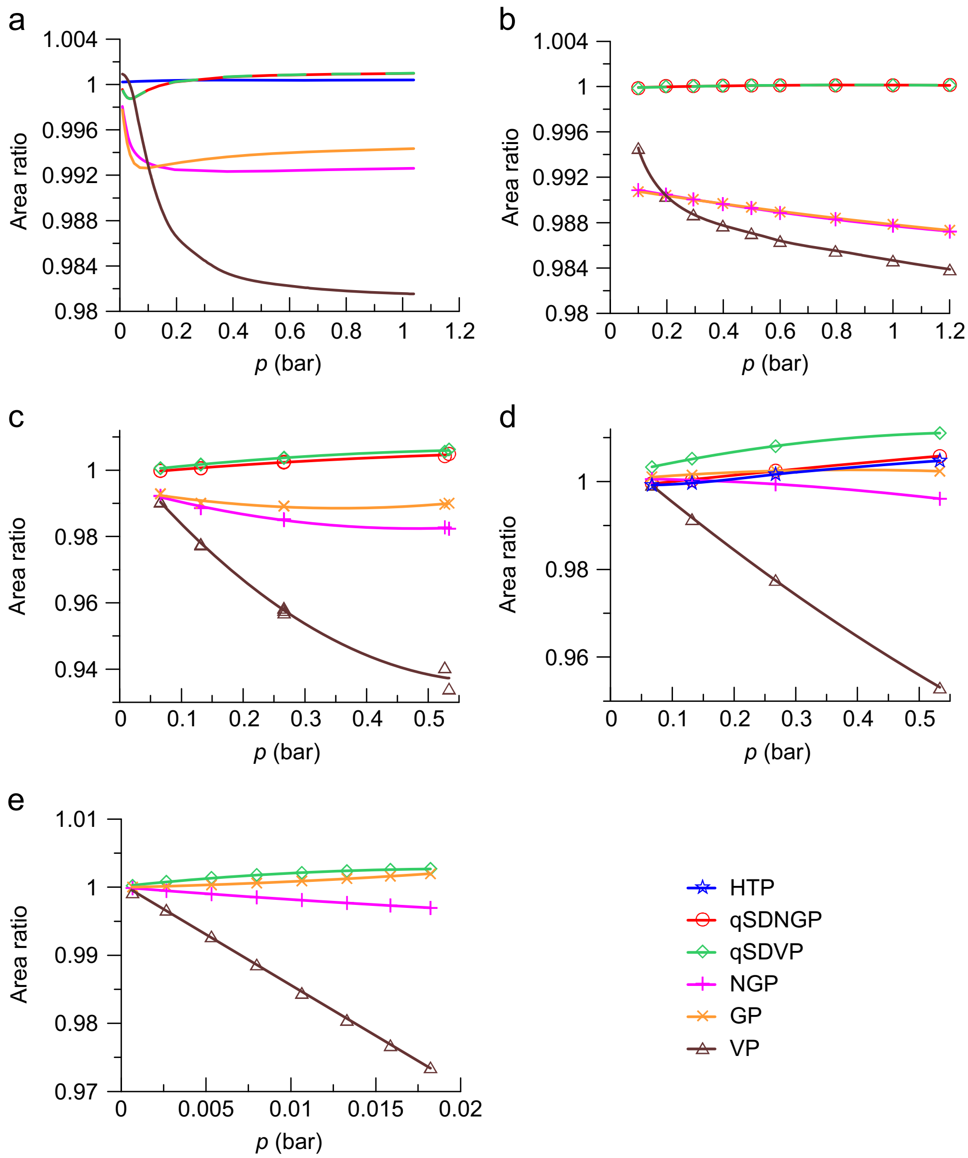

Fig. 8. Ratio of the fitted line area to the reference (the most accurate) area vs. perturber pressure, obtained from multi-spectrum fits of (a) simulated spectra of H_2O ν_3 $4_{04}-3_{03}$ line perturbed by N_2, the reference areas are exact; (b) measured spectra of H_2O ν_3 $4_{04}-3_{03}$ line perturbed by N_2, the reference areas are from the HTP fits (c) measured spectra of H_2O $2\nu_1+\nu_3$ $4_{04}-3_{03}$ line perturbed by N_2, the reference areas are from the HTP fits; (d) measured spectra of H_2O $2\nu_1+\nu_3$ $4_{04}-3_{03}$ line perturbed by SF_6, the reference areas are from the pChSDNGP fits; (e) measured spectra of self-broadened H_2O $4\nu_2$ $5_{14}-5_{05}$ line, the reference areas are from the qSDNGP fits.

residuals to less than 0.05%. Moreover, multi-spectrum fits of the HTP to measured N_2-broadened H_2O lines did not reveal any systematic deviations. The simulations in Fig. 2 suggest that a SNR higher than 4000 and a wide range of Γ/Γ_D is needed in the multi-spectrum fit procedure to clearly distinguish between the HTP and measured spectra. On the other hand, the results shown in Fig. 3 suggest that if the pressure range of the measured spectra is sufficient to cover both the Doppler and collisional regimes then all parameters of the HTP can be properly obtained from the multi-spectrum fit even if SNR of spectra is lower than 1000. This is also confirmed by the reasonably low uncertainties of the fitted HTP parameters for the $2\nu_1+\nu_3 4_{04}-3_{03}$ line in Table 1. However, even at very high SNR the fitted parameters ν_{opt}, a_W, and η of the HTP can be systematically different by even 20% for different ranges of Γ/Γ_D ratios in the measured spectra.

For the case of perturbation by heavy SF_6 the quadratic speed-dependence model used in the HTP is clearly not sufficient to properly describe measured spectra at a SNR of about 500. In this case the hypergeometric speed-dependence model leads to significant improvement in the fit quality.

It should be noted here that although the HTP leads to a very good agreement with the calculated H_2O line

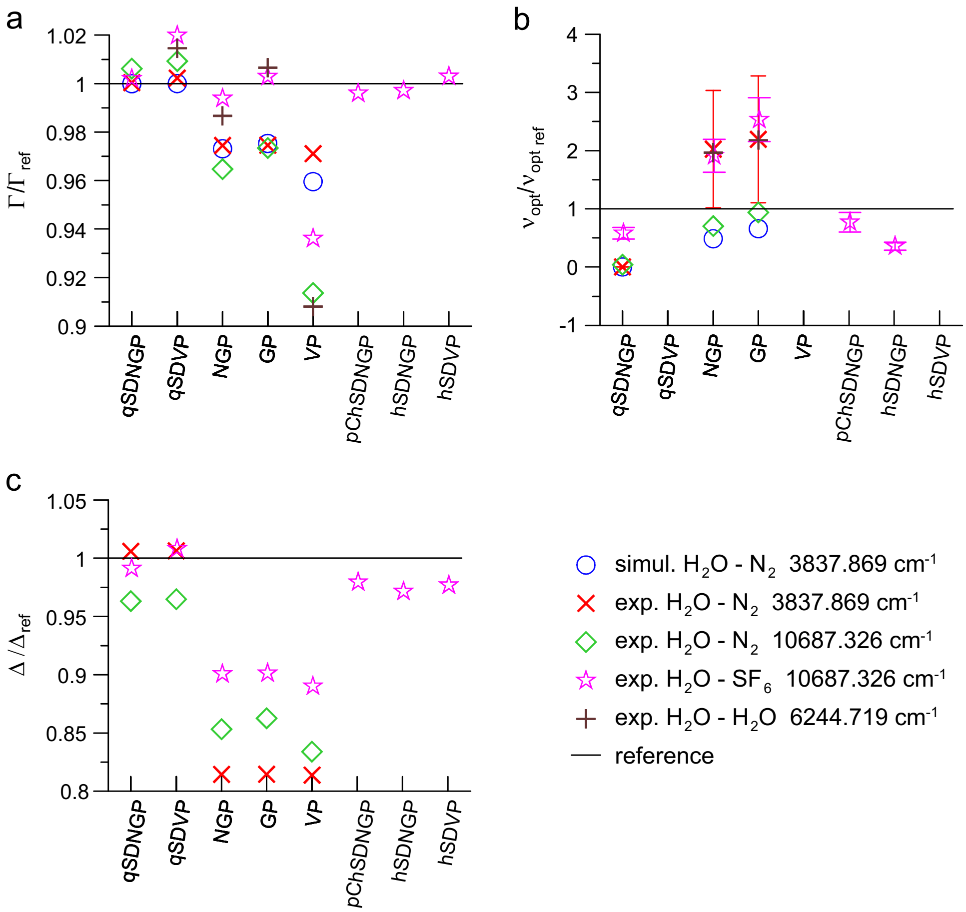

Fig. 9. Ratios of the line shape coefficients: (a) collisional broadening parameter Γ/p; (b) frequency of optical collisions ν_{opt}/p; (c) collisional shifting parameter Δ/p, obtained from the multi-spectrum fits of various line shape models, to the corresponding coefficient Γ_{ref}, $\nu_{opt_{ref}}$, Δ_{ref} obtained from the reference model HTP. For the self-broadened H_2O line the reference model is the qSDNGP. Standard uncertainties of parameters are indicated only if larger than symbols.

Table 1
Line shape parameters obtained from multi-spectrum fits of the HTP to simulated and experimental H_2O spectra: collisional broadening parameter Γ/p, collisional narrowing parameter ν_{opt}/p, quadratic speed-dependence of collisional broadening a_W and shifting a_S parameters, correlation parameter η. The collisional shift coefficients Δ/p of $2\nu_1+\nu_3$ $4_{04}-3_{03}$ line were constrained to previously reported values [21]. Unperturbed transition wavenumbers are from HITRAN [30]. Γ/p, ν_{opt}/p and Δ/p are in units (kHz/Pa). These values can be converted to more commonly used units using the conversion 1 cm^{-1} atm^{-1}=295.872 kHz Pa^{-1}.

Band and line	ν_0 (cm^{-1})	Perturber	Γ/p	ν_{opt}/p	a_W	a_S	η	Δ/p
ν_3 $4_{04}-3_{03}$ simul.	3837.86925	N_2	31.6089(12)	15.930(15)	0.1843(2)	–	0.550(1)	–
ν_3 $4_{04}-3_{03}$	3837.86925	N_2	31.48(15)	7.1(18)	0.164(11)	0.79(24)	0.24(12)	0.547(27)
$2\nu_1+\nu_3$ $4_{04}-3_{03}$	10,687.361176	N_2	31.63(6)	14.8(12)	0.198(6)	0.55(12)	0.49(4)	−1.66(16)
$2\nu_1+\nu_3$ $4_{04}-3_{03}$	10,687.361176	SF_6	25.65(6)	4.7(9)	0.124(6)	0.40(6)	0.08(3)	−10.49(16)
$4\nu_2$ $5_{14}-5_{05}$	6244.71929(19)	H_2O	130.3(14)	17.22(22)	0.0677(8)	−0.11(17)	-	3.6(54)

ν_3 4_{04}-3_{03} perturbed by N_2 (shown in Fig. 1), we have tested that replacing the quadratic speed-dependence model to the hypergeometric one leads to further reduction (about two times) of the fit residuals.

Finally, it is clear from results shown in Fig. 9 that line-shape parameters Γ/p, ν_{opt}/p, a_W, and η retrieved from fits of one of the profiles considered here cannot be directly used in another profile if a sub-percent level of accuracy is expected. Incorporation of high-accuracy measured line-shape parameters into spectroscopic databases based on the HTP requires fitting the data with HTP rather than converting parameters retrieved from different profiles. However, to make use of spectra with insufficiently high SNR or a too-limited range of Γ/Γ_D one could set some parameters, e.g. η, a_S to zero, to enable fit convergence and to preserve compatibility with the HTP.

Acknowledgments

Drs. D. Mondelain, S. Kassi and A. Campargue (LIPhy, Grenoble) are gratefully acknowledged for providing CRDS spectra of pure H_2O. The research is part of the program of the National Laboratory FAMO in Toruń, Poland, and is supported by the Polish National Science Centre Projects nos. DEC-2011/01/B/ST2/00491 and DEC-2013/11/D/ST2/02663. The research is also supported by the Foundation for Polish Science TEAM Project co-financed by the EU European Regional Development Fund. A. Cygan is partially supported by the Foundation for Polish Science START Project. Dr. Hodges is supported by the Greenhouse Gas and Climate Sciences Measurement Program of the National Institute of Standards and Technology. Drs. Bermejo and Domenech have been supported by Grants CSD2009-00038 (Consolider Astromol) and FIS2012-38175 from the Spanish Ministry of Economy and Competitiveness.

References

[1] Ngo NH, Lisak D, Tran H, Hartmann J-M. An isolated line-shape model to go beyond the Voigt profile in spectroscopic databases and radiative transfer codes. J Quant Spectrosc Radiat Transfer 2013;129:89–100. http://dx.doi.org/10.1016/j.jqsrt.2013.05.034.

[2] Ngo NH, Lisak D, Tran H, Hartmann J-M. Erratum to "An isolated line-shape model to go beyond the Voigt profile in spectroscopic databases and radiative transfer codes" [J Quant Spectrosc Radiat Transf 129 (2013) 89–100]. J Quant Spectrosc Radiat Transfer 2014;134:105. http://dx.doi.org/10.1016/j.jqsrt.2013.10.016.

[3] Tran H, Ngo NH, Hartmann J-M. Efficient computation of some speed-dependent isolated line profiles. J Quant Spectrosc Radiat Transfer 2013;129:199–203. http://dx.doi.org/10.1016/j.jqsrt.2013.06.015.

[4] Tran H, Ngo NH, Hartmann J-M. Erratum to "Efficient computation of some speed-dependent isolated line profiles" [J Quant Spectrosc Radiat Transf 129 (2013) 199–203]. J Quant Spectrosc Radiat Transfer 2014;134:104.http://dx.doi.org/10.1016/j.jqsrt.2013.10.015.

[5] Pine AS. Asymmetries and correlations in speed-dependent Dicke-narrowed line shapes of argon-broadened HF. J Quant Spectrosc Radiat Transf 1999;62:397–423.

[6] Rohart F, Mader H, Nicolaisen H-W. Speed dependence of rotational relaxation induced by foreign gas collisions: studies on CH_3F by millimeter wave coherent transients. J Chem Phys 1994;101:6475–86. http://dx.doi.org/10.1063/1.468342.

[7] Priem D, Rohart F, Colmont J-M, Wlodarczak G, Bouanich J-P. Lineshape study of the $J=3$łeftarrow2 rotational transition of CO perturbed by N_2 and O_2. J Mol Struct 2000;517:435–54. http://dx.doi.org/10.1016/S0022-2860(99)00268-9.

[8] Tennyson J, Bernath PF, Campargue A, Csaszar AG, Daumont L, Gamache RR, et al. Recommended isolated-line profile for representing high-resolution spectroscopic transitions. Pure Appl Chem 2014;86:1931–43. http://dx.doi.org/10.1515/pac-2014-0208.

[9] Cygan A, Lisak D, Wójtewicz S, Domysławska J, Hodges JT, Trawiński RS, et al. High signal-to-noise ratio laser technique for accurate measurements of spectral line parameters. Phys Rev A 2012;85:022508. http://dx.doi.org/10.1103/PhysRevA.85.022508.

[10] de Vizia MD, Castrillo A, Fasci E, Amodio P, Moretti L, Gianfrani L. Experimental tests of the quadratic approximation in the partially correlated speed-dependent hard-collision profile. Phys Rev A 2014;90:022503. http://dx.doi.org/10.1103/PhysRevA.90.022503.

[11] Long DA, Truong GW, van Zee RD, Plusquellic DF, Hodges JT. Frequency-agile rapid scanning spectroscopy: absorption sensitivity of $2\times10^{-12}\,cm^{-1}\,Hz^{1/2}$ with a tunable diode laser. Appl Phys B 2014;114:489–95. http://dx.doi.org/10.1007/s00340-013-5548-5.

[12] Crisp D, Atlas RM, Breon F-M, Brown LR, Burrows JP, Ciais P, et al. The Orbiting Carbon Observatory (OCO) mission. Adv Space Res 2004;34:700–9.

[13] Miller CE, Brown LR, Toth RA, Benner DC, Devi VM. Spectroscopic challenges for high accuracy retrievals of atmospheric CO_2 and the Orbiting Carbon Observatory (OCO) experiment. C R Phys 2005;6:876–87.

[14] Miller CE, Crisp D, DeCola PL, Olsen SC, Randerson JT, Michalak AM, et al. Precision requirements for space-based data. J Geophys Res 2007;112:D10314. http://dx.doi.org/10.1029/2006JD007659.

[15] Thompson DR, Chris Benner D, Brown LR, Crisp D, Malathy Devi V, Jiang Y, et al. Atmospheric validation of high accuracy CO_2 absorption coefficients for the OCO-2 mission. J Quant Spectrosc Radiat Transf 2012;113:2265–76.

[16] Bui TQ, Long DA, Cygan A, Sironneau VT, Hogan DW, Rupasinghe PM, et al. Observations of Dicke narrowing and speed dependence in air-broadened CO_2 lineshapes near 2.06 μm. J Chem Phys 2014;141:174301. http://dx.doi.org/10.1063/1.4900502.

[17] Sironneau VT, Hodges JT. Line shapes, positions and intensities of water transitions near 1.28 μm. J Quant Spectrosc Radiat Transf 2015:1–15.

[18] Wcisło P, Lisak D, Ciuryło R, Pine AS. In preparation.

[19] Ngo NH, Tran H, Gamache RR, Bermejo D, Domenech J-L. Influence of velocity effects on the shape of N_2 (and air) broadened H_2O lines revisited with classical molecular dynamics simulations. J Chem Phys 2012;137:0643028. http://dx.doi.org/10.1063/1.4739467.

[20] Tran H, Bermejo D, Domenech J-L, Joubert P, Gamache RR, Hartmann J-M. Collisional parameters of H_2O lines: velocity effects on the line-shape. J Quant Spectrosc Radiat Transf 2007;108:126–45. http://dx.doi.org/10.1016/j.jqsrt.2007.03.009.

[21] Lisak D, Hodges JT, Ciurylo R. Comparison of semiclassical line-shape models to rovibrational H_2O spectra measured by frequency-stabilized cavity ring-down spectroscopy. Phys Rev A 2006;73:012507. http://dx.doi.org/10.1103/PhysRevA.73.012507.

[22] Ward J, Cooper J, Smith EW. Correlation effects in the theory of combined Doppler and pressure broadening—I. Classical theory. J Quant Spectrosc Radiat Transf 1974;14:555–90. http://dx.doi.org/10.1016/0022-4073(74)90036-3.

[23] Tran H, Ngo NH, Hartmann J-M, Gamache RR, Mondelain D, Kassi S, et al. Velocity effects on the shape of pure H_2O isolated lines: complementary tests of the partially correlated speed-dependent Keilson–Storer model. J Chem Phys 2013;138:034302. http://dx.doi.org/10.1063/1.4774094.

[24] Ciuryło R, Jaworski R, Jurkowski J, Pine AS, Szudy J. Spectral line shapes modeled by a quadratic speed-dependent Galatry profile. Phys Rev A 2001;63:032507. http://dx.doi.org/10.1103/PhysRev-A.63.032507.

[25] Rohart F, Wlodarczak G, Colmont J-M, Cazzoli G, Dore L, Puzzarini C. Galatry versus speed-dependent Voigt profiles for millimeter lines of O_3 in collision with N_2 and O_2. J Mol Spectrosc 2008;251:28292. http://dx.doi.org/10.1016/j.jms.2008.03.005.

[26] de Vizia MD, Castrillo A, Fasci E, Moretti L, Rohart F, Gianfrani L. Speed dependence of collision parameters in the H_2^{18} O near-IR spectrum: experimental test of the quadratic approximation. Phys Rev A 2012;85:062512. http://dx.doi.org/10.1103/PhysRevA.85.062512.

[27] Hodges JT, Lisak D, Lavrentieva N, Bykov A, Sinitsa L, Tennyson J, et al. Comparison between theoretical calculations and high-resolution measurements of pressure broadening for near-infrared water spectra. J Mol Spectrosc 2008;249:86–94. http://dx.doi.org/10.1016/j.jms.2008.02.022.

[28] Wójtewicz S, Lisak D, Cygan A, Domysławska J, Trawiński RS, Ciuryło R. Line-shape study of self-broadened O_2 transitions measured by Pound–Drever–Hall-locked frequency-stabilized cavity ring-down spectroscopy. Phys Rev A 2011;84:032511. http://dx.doi.org/10.1016/10.1103/PhysRevA.84.032511.

[29] Lisak D, Havey DK, Hodges JT. Spectroscopic line parameters of water vapor for rotation–vibration transitions near 7180 cm^{-1}. Phys Rev A 2009;79:052507. http://dx.doi.org/10.1103/Phys-RevA.79.052507.

[30] Rothman LS, Gordon IE, Babikov Y, Barbe A, Chris Benner D, Bernath PF, et al. The HITRAN 2012 molecular spectroscopic database. J Quant Spectrosc Radiat Transfer 2013;130:4–50 http://dx.doi.org/10.1016/j.jqsrt.2013.07.002.